Bistability in Pulse Propagation in Networks of Excitatory and Inhibitory Populations

David Golomb
Zlotowski Center for Neuroscience and Department of Physiology, Faculty of Health Sciences, Ben Gurion University of the Negev, Be'er-Sheva 84105, Israel

G. Bard Ermentrout
Department of Mathematics, University of Pittsburgh, Pittsburgh, Pennsylvania 15260
(Received 13 July 2000)

We study the propagation of traveling solitary pulses in one-dimensional networks of excitatory and inhibitory integrate-and-fire neurons. Slow pulses, during which inhibitory cells fire well before neighboring excitatory cells, can propagate along the network at intermediate inhibition levels. At higher levels, they destabilize via a Hopf bifurcation. There is a bistable parameter regime in which both fast and slow pulses can propagate. Lurching pulses with spatiotemporal periodicity can propagate in regimes for which continuous pulses do not exist.

DOI: 10.1103/PhysRevLett.86.4179 PACS numbers: 87.19.La, 05.45.–a, 87.10.+e

Theoretical work on pulse propagation has dealt mainly with networks of purely excitatory neurons [1–4]. Such networks exhibit only fast, epileptic pulses, with velocity that cannot be slower than about 6 cm/s [1,5–7]. Experimental studies, however, have emphasized the importance of inhibition in shaping the form and velocity of the pulses in cortical tissues and even preventing their propagation [8–10]. Furthermore, recent experimental evidence shows that with inhibition intact, certain types of stimulation lead to the propagation of slow (<1 cm/s) pulses in normal cortical tissues [11,12]. These pulses may account for the generation of a subset of cortical rhythms during sleep. Propagating neuronal activity takes part in shaping visual receptive fields, and hence affects information processing in the brain [13]. It is also important in communication in some invertebrates, notably, the coelenterates [14].

The goal of this work is to explore theoretically the effects of inhibition on the form and velocity of propagating pulses in networks of excitable cells [15], such as cortical networks. Using a simplified version of the integrate-and-fire neuronal model, we calculate exactly the velocity and stability of propagating continuous traveling pulses. We find two types of propagating pulses, which differ by their velocities and by the delays between the firing times of inhibitory and excitatory cells: (1) "Fast" pulses, which are similar to the pulses observed with no inhibition. During such a pulse, an inhibitory cell fires after or slightly before its neighboring excitatory cells. (2) "Slow" pulses, in which inhibitory cells lead considerably in firing, whereas excitatory cells "push" the pulse from behind. As inhibition increases, there may be a crossover between the two pulse types, or there may be a bistable regime, in which both types of pulse can propagate and selection is made by initial conditions. Moreover, if the excitatory-to-excitatory synaptic connections are slow, a domain of parameters exists where these continuously propagating pulses do not exist. Instead, discontinuous pulses with spatiotemporal periodicity propagate. These pulses were denoted "lurching pulses" [4,16]. This work is devoted to study propagation of neuronal activity into a silent regime. Propagation of "phase waves" within an active region is described in Ref. [17].

We consider a one-dimensional network of excitatory (E) and inhibitory (I) neurons. Each neuron is described by its membrane potential $V_\alpha(x,t)$, $\alpha = E, I$, and its dynamics is governed by the integrate-and-fire scheme in the excitable regime [3]

$$\frac{\partial V_\alpha(x,t)}{\partial t} = -\frac{V_\alpha(x,t)}{\tau_{0\alpha}} + I_{\mathrm{syn},E\alpha}(x,t) - I_{\mathrm{syn},I\alpha}(x,t). \tag{1}$$

Here $\tau_{0\alpha}$ is the passive membrane time constant of the neuron, and $I_{\mathrm{syn},\beta\alpha}$ is the synaptic current through which the neurons are coupled. When the membrane potential of a neuron V reaches a threshold $V_{T\alpha}$, the neuron fires a spike, after which it is silent forever. In the following, we denote by $T_\alpha(x)$ the time at which a neuron located at x fires. The network architecture is shown in Fig. 1. The synaptic current $I_{\mathrm{syn},\beta\alpha}$ is

$$I_{\mathrm{syn},\beta\alpha}(x,t) = g_{\beta\alpha}\int_{-\infty}^{\infty} dx'\, w_{\beta\alpha}(x-x') \times \alpha_{\beta\alpha}[t - T_\beta(x')], \tag{2}$$

where $g_{\beta\alpha}$ is the synaptic coupling strength from the β population to the α population. A presynaptic spike induces a postsynaptic current in the form $\alpha_{\beta\alpha}(t) = \exp(-t/\tau_{s\beta\alpha})$ if $t > 0$ and 0 otherwise. The spatial dependence of the synaptic strength on distance ("synaptic footprint shape") is given by $w_{\beta\alpha}(x) = (2\sigma_{\beta\alpha})^{-1} \times \exp(-|x|/\sigma_{\beta\alpha})$.

In order to analyze the dynamics, we define the Green's function $G_{\beta\alpha}(t)$ for $t > 0$ as $dG_{\beta\alpha}/dt = -G_{\beta\alpha}/\tau_{0\alpha} + \alpha_{\beta\alpha}(t)$ and $G_{\beta\alpha}(t < 0) = 0$, and we obtain the following

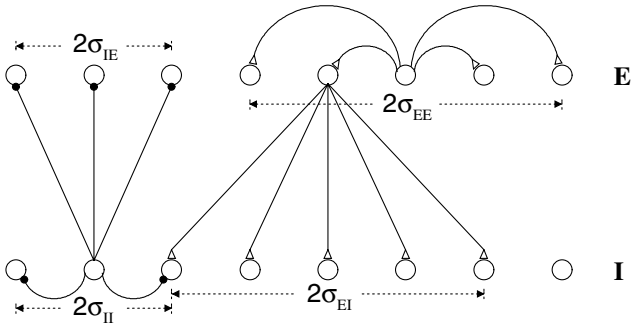

FIG. 1. Synaptic architecture of the model. The coupling between cells decays with distance, with characteristic decay lengths denoted by σ's; the first and second letters in the subscript denote the pre- and postsynaptic populations, respectively.

for $t > 0$: $G_{\beta\alpha}(t) = \tau_{0\alpha}/(\tau_{0\alpha} - \tau_{s\beta\alpha})[\exp(-t/\tau_{0\alpha}) - \exp(-t/\tau_{s\beta\alpha})]$. The integrated form of Eqs. (1) and (2) is given by the two equations for $\alpha = E, I$:

$$V_{T\alpha} = \sum_{\beta=E,I} s_\beta g_{\beta\alpha} \times \int_{-\infty}^{\infty} dx' \, w_{\beta\alpha}(x') G_{\beta\alpha}[T_\alpha(x) - T_\beta(x - x')], \quad (3)$$

where $s_E = 1$ and $s_I = -1$. In addition, the neuronal voltage should not exceed 1 before spiking: $V_\alpha(x,t) < V_{T\alpha}$ for all $t < T_\alpha(x)$. A necessary, but not sufficient, condition for this is

$$\frac{dV_\alpha[x, T(x)]}{dt} > 0 . \quad (4)$$

We consider a traveling pulse solution with velocity ν, with an inhibitory cell's firing time lagging after the firing time of the excitatory cell at the same position by ζ:

$$T_E(x) = \frac{x}{\nu}, \qquad T_I(x) = \frac{x}{\nu} + \zeta . \quad (5)$$

Negative ζ means that an I cell fires before a neighboring E cell. Substituting Eq. (5) in Eq. (3) yields

$$V_{T\alpha} = B_{E\alpha} - B_{I\alpha} , \quad (6)$$

where

$$B_{\beta\alpha} = g_{\beta\alpha} \int_0^\infty dx \, w_{\beta\alpha}(x + \zeta\nu s_{\beta\alpha}) G_{\beta\alpha}\left(\frac{x}{\nu}\right). \quad (7)$$

We define $s_{\beta\alpha} = (s_\alpha - s_\beta)/2$. Substituting the expressions for $G_{\beta\alpha}$ and $w_{\beta\alpha}$ in Eqs. (6) and (7), we obtain two algebraic equations for ν and ζ, for negative ζ

$$V_{TE} = g_{EE} \frac{\tau_{0E}\nu\sigma_{EE}}{2(\nu\tau_{0E} + \sigma_{EE})(\nu\tau_{sEE} + \sigma_{EE})} - g_{IE} \frac{\tau_{0E}\nu}{(\tau_{0E} - \tau_{sIE})} \times \left[\frac{\tau_{0E}^2\nu}{\nu^2\tau_{0E}^2 - \sigma_{IE}^2} \exp\left(\frac{\zeta}{\tau_{0E}}\right) - \frac{\tau_{sIE}^2\nu}{\nu^2\tau_{sIE}^2 - \sigma_{IE}^2} \exp\left(\frac{\zeta}{\tau_{sIE}}\right) + \frac{(\tau_{0E} - \tau_{sIE})\sigma_{IE}}{2(\nu\tau_{0E} - \sigma_{IE})(\nu\tau_{sIE} - \sigma_{IE})} \exp\left(\frac{\zeta\nu}{\sigma_{IE}}\right) \right], \quad (8)$$

$$V_{TI} = g_{EI} \frac{\tau_{0I}\nu\sigma_{EI}}{2(\nu\tau_{0I} + \sigma_{EI})(\nu\tau_{sEI} + \sigma_{EI})} \exp\left(\frac{\zeta\nu}{\sigma_{EI}}\right) - g_{II} \frac{\tau_{0I}\nu\sigma_{II}}{2(\nu\tau_{0I} + \sigma_{II})(\nu\tau_{sII} + \sigma_{II})} . \quad (9)$$

Equations in a similar form are obtained for positive ζ.

Stability of the continuous pulses is calculated by following the growth rate of a small perturbation $T_E(x) = x/\nu + \theta_E(x)$, $T_I(x) = x/\nu + \zeta + \theta_I(x)$. Assuming that the perturbation evolves as $\exp(\lambda x)$, we find that the continuous pulse is stable if all the solutions of the characteristic equation $\det[A(\lambda)] = 0$ have negative real parts, where the components of the 2×2 matrix A are

$$A_{\beta\alpha} = -s_\beta B'_{\beta\alpha}(\lambda) + [B'_{E\alpha}(0) - B'_{I\alpha}(0)]\delta_{\alpha\beta} , \quad (10)$$

where

$$B'_{\beta\alpha}(\lambda) = g_{\beta\alpha} \exp(-\lambda\zeta\nu s_{\beta\alpha}) \times \int_0^\infty dx \, w_{\beta\alpha}(x + \zeta\nu s_{\beta\alpha}) G'_{\beta\alpha}\left(\frac{x}{\nu}\right) e^{-\lambda x} \quad (11)$$

and $G'(t) = dG(t)/dt$. Note that $\lambda = 0$ is always a solution of the characteristic equation because of the translation invariance. A pulse can lose stability at a saddle-node bifurcation (SNB), where $d\{\det[A(\lambda)]\}/d\lambda|_{\lambda=0} = 0$, or at a Hopf bifurcation (HB), where $\lambda = i\omega$.

The dependence of ν on g_{IE} is shown in Figs. 2(a)–2(c) for three values of g_{EI}. At low g_{EI} values, there is only one stable branch of fast pulses, which terminates at a SNB. At large g_{EI} values, there is a crossover between fast pulses and slow pulses as g_{IE} increases. At intermediate g_{EI} values, bistability exists, and at intermediate g_{IE} values, both the fast pulse and the slow pulse can propagate. The time difference ζ increases as ν decreases, and therefore the I cell time lead is larger for the slow pulse than for the fast pulse. In order to illustrate the behavior of the two types of pulses, we present, in Fig. 3(a), rastergrams (neuronal firing times) obtained from simulating Eqs. (1) and (2). The velocity of the faster pulse is larger than the velocity of the slower pulse by an order of magnitude. Whereas during the fast pulse (I), E cells fire before or slightly after the I cells, E cells fire well after the I cells during the slow pulse (II). This pulse can be viewed as a front of I-cells' spikes pushed from behind by the E-cells' spikes; because each E cell receives strong inhibition from neurons in front of it, the pulse propagates slowly.

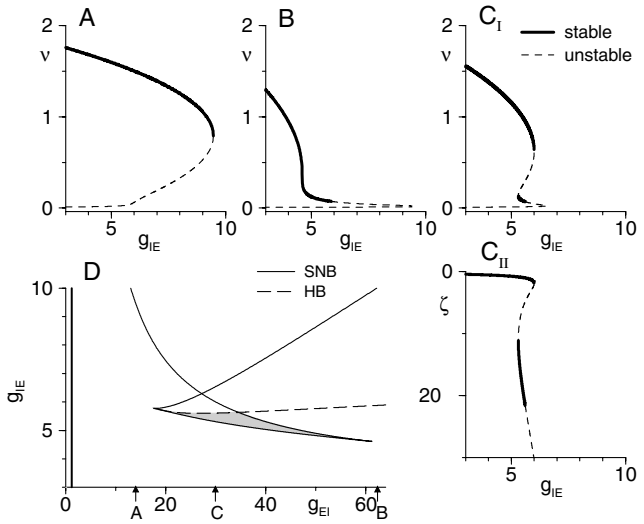

FIG. 2. (a)–(c): The velocity ν (in units of 1/ms) of the continuous pulse as a function of g_{IE} for $g_{EI} = 14$ (a), $g_{EI} = 62$ (b), and $g_{EI} = 30$ (c). In (c), the value of ζ (in units of ms) is also plotted. Solid lines denote stable pulses, and dashed lines denote unstable pulses. There is another, extremely unstable, branch with very small ν and large, positive ζ which is not shown. (d) Two-parameter (g_{EI}-g_{IE}) bifurcation diagram. Saddle-node bifurcations are denoted by a narrow solid line, and Hopf bifurcations are denoted by a dashed line. Bistability exists in the shaded regime. For g_{EI} values smaller than the values on the wide solid line on the left, pulses propagate only among excitatory cells, whereas inhibitory cells remain silent. The parameters σ's and g's are measured in dimensionless units, $V_{TE} = V_{TI} = 1$. Parameters are as follows: $\tau_0 E = \tau_0 I = 30$ ms, $\tau_{sEE} = \tau_{sEI} = 2.5$ ms, $\tau_{sIE} = \tau_{sII} = 8$ ms, $g_{EE} = 12$, $\sigma_{EE} = 1$, $\sigma_{IE} = 0.9$, $\sigma_{EI} = 0.8$, $g_{II} = 2$, $\sigma_{II} = 0.5$.

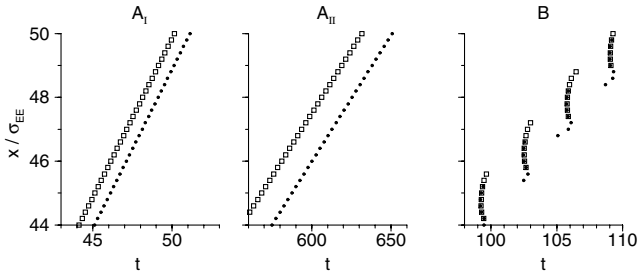

FIG. 3. Rastergrams obtained by simulations of the neuronal dynamics; firing times of excitatory cells are denoted by solid circles, and firing times of inhibitory cells are denoted by open squares. There are 50 neurons from each type within one unit length, and spikes of only one out of every 10 neurons are plotted. The pulses were initiated by initiating a pulse in a group of neurons with $x < 10$ with ν and ζ calculated from the theory [in (a)] or as a "shock" for $x < 0.5$ [in (b)] [4]. Two types of continuous pulses are shown in A_I and A_{II} for the different initial conditions (note the difference in time scale), whereas a lurching pulse is shown in (b). Parameters for (a) are as in Fig. 2(c); $g_{IE} = 5.5$. Parameters that are different in (b) are as follows: $\tau_{sEE} = 50$ ms, $\tau_{sEI} = 2$ ms, $\tau_{sIE} = \tau_{sII} = 5$ ms, $g_{EE} = 250$, $g_{IE} = 21$, $\sigma_{IE} = 0.7$, $g_{EI} = 20$, $g_{II} = 17$.

The slow pulses lose stability at a HB, as shown in Figs. 2(b) and 2(c). Whereas our theory cannot determine what happens for g_{IE} larger than its value at the HB, extensive numerical simulations indicate that no pulse can propagate in that regime. This is in contrast to the effect of synaptic delay in excitatory networks [4], in which the destabilization due to a HB leads to discontinuous, lurching pulses. The bistable regime, in which both fast and slow pulses can propagate, is denoted by shading in the two-parameter diagram [Fig. 2(d)]. It is bounded by two codimension-2 cusp bifurcations [18]. The cusp at low g_{EI} produces the slow pulse branch as a "ripple" on an unstable solution, and the cusp at high g_{EI} connects the slow and the fast branches.

Both the fast and slow pulses are continuous. Can pulses with more complicated spatiotemporal form be obtained in our model? We find such lurching pulse [4], with spatiotemporal periodicity in the firing pattern, if the E-to-E excitation is made slow, whereas all the other synapses decay fast. A typical rastergram of a lurching pulse is shown in Fig. 3(b); the parameter set is characterized by a slow τ_{sEE} (50 ms). A group of E cells that fire inhibit other excitatory neurons through the neighboring inhibitory neurons, but the E-to-E excitation is prolonged enough to recruit a new group of excitatory cells into the pulse at a later time. Surprisingly, during a lurching pulse, the firing time of the spikes is not a monotone function of the spatial position [see Fig. 3(b)]. As the parameter g_{IE} increases, the system switches from a continuous to a lurching pulse, although not through instability. Instead, the continuous pulse ceases to exist because the voltages $V_I(t, x)$ and $V_E(t, x)$ are larger than 1 for $t < T_I(x, t)$ and $t < T_E(x, t)$, respectively [19], Eq. (4) does not hold, and a lurching pulse emerges. At even higher g_{IE} values, no pulse can propagate.

To conclude, our analysis of the existence, velocity, and stability of continuous pulses in one-dimensional two-population networks has revealed several unexpected results. (1) Slow pulses, during which inhibitory neurons fire well before excitatory neurons, are observed. Such slow pulses are not seen in neuronal networks with excitation only [20–22], because the mechanism of their generation requires leading inhibition. (2) These pulses can coexist with fast pulses, during which the two cell types fire nearly together. Such bistability has not been observed in models of spatially extended one-dimensional excitable systems with diffusive coupling [23–25]. (3) With slow E-to-E excitation, lurching pulses are displayed in a regime where continuous pulses do not exist. The slow pulses and the bistability were found in cases of finite axonal delays, and in networks in which the integrate-and-fire scheme was replaced by the Morris-Lecar model, a version of a conductance-based model [26]. Furthermore, slow pulses with inhibitory cells leading in firing are observed even if neurons are allowed to fire many spikes. We observed these pulses in a conductance-based network model in which

excitatory cells and excitatory synaptic variables were represented by the scheme described in [1], and inhibitory cells and inhibitory synaptic variables were represented by the scheme described in [27]. The appearance of slow pulses in several different models demonstrates the generality of this phenomenon.

Our theory yields two predictions that can be tested in neurobiological experiments on cortical slices: (1) Inhibitory cells fire well before excitatory cells during the slow pulse. This prediction can be tested by dual recording from neighboring excitatory and inhibitory cells during experimentally induced slow pulses [11,12]. (2) There is a sharp transition from a slow pulse to a fast pulse as inhibition is blocked. This prediction can be tested by measuring the pulse velocity as inhibition is gradually blocked. Work in this direction is in progress. Detailed description of the calculations will be given elsewhere.

We are thankful to E. Meron, J. Rinzel, M. J. Gutnick, and J.-Y. Wu for helpful discussions. This research was supported by Grant No. 9800015 from the United States-Israel Binational Science Foundation (BSF), Jerusalem, Israel, to D. G. and G. B. E.; G. B. E. is funded by NSF and NIMH.

[1] D. Golomb and Y. Amitai, J. Neurophysiol. **78**, 1199–1211 (1997).
[2] G. B. Ermentrout, J. Comput. Neurosci. **5**, 191–208 (1998).
[3] P. C. Bressloff, Phys. Rev. Lett. **82**, 2979–2982 (1999).
[4] D. Golomb and G. B. Ermentrout, Proc. Natl. Acad. Sci. U.S.A. **96**, 13 480–13 485 (1999); Network **11**, 221–246 (2000).
[5] H. Petsche, O. Prohaska, P. Rappelsberger, R. Vollmer, and A. Kaiser, Epilepsia **15**, 439–463 (1974).
[6] R. D. Traub, J. G. R. Jefferys, and R. Miles, J. Physiol. London **472**, 267–287 (1993).
[7] R. D. Chervin, P. A. Pierce, and B. W. Connors, J. Neurophysiol. **60**, 1695–1713 (1988).
[8] Y. Chagnac-Amitai and B. W. Connors, J. Neurophysiol. **62**, 1149–1162 (1989).
[9] J.-Y. Wu, L. Guan, and Y. Tsau, J. Neurosci. **19**, 5005–5015 (1999).
[10] N. Laaris, G. C. Carlson, and A. Keller, J. Neurosci. **20**, 1529–1537 (2000).
[11] J.-Y. Wu and L. Guan, J. Neurophysiol. (to be published).
[12] M. V. Sanchez-Vives and D. A. McCormick, Nature Neurosci. **3**, 1027–1034 (2000).
[13] V. Bringuier, F. Chavane, L. Glaeser, and Y. Fregnac, Science **283**, 695–699 (1999).
[14] T. H. Bullock and G. A. Horridge, *Structure and Function in the Nervous Systems of Invertebrates* (W. H. Freeman, San Francisco, 1965), Vol. 1.
[15] Experimental [e.g., U. Kim, T. Bal, and D. A. McCormick, J. Neurophysiol. **84**, 1301–1323 (1995)] and theoretical [e.g., D. Golomb, X.-J. Wang, and J. Rinzel, J. Neurophysiol. **75**, 750–769 (1996)] work has been dedicated to thalamic networks composed of excitatory and inhibitory neurons. Thalamic excitatory cells possess the postinhibitory rebound mechanism that causes them to respond to inhibition as "excitation with delay" [4,16], and therefore these networks have completely different dynamics than the networks described here.
[16] J. Rinzel, D. Terman, X.-J. Wang, and B. Ermentrout, Science **279**, 1351–1355 (1998).
[17] G. B. Ermentrout and D. Kleinfeld, Neuron **29**, 33–44 (2001).
[18] F. C. Hoppensteadt and E. M. Izhikevich, *Weakly Connected Neural Networks* (Springer-Verlag, New York, 1997).
[19] For the parameter set of Fig. 3, there is a narrow regime between $g_{IE} = 19$ and $g_{IE} = 19.7$ in which the continuous pulse loses stability and then gains it back via two consecutive HB, before it ceases to exist at $g_{IE} = 20.6$.
[20] W. M. Kistler, R. Seitz, and J. L. van Hemmen, Physica (Amsterdam) **114D**, 273–295 (1998).
[21] D. Horn and I. Opher, Philos. Mag. B **77**, 1575–1583 (1998).
[22] C. Fohlmeister, W. Gerstner, R. Ritz, and J. L. van Hemmen, Neural Comput. **7**, 905–914 (1995).
[23] M. C. Cross and P. C. Hohenberg, Rev. Mod. Phys. **65**, 851–1112 (1993).
[24] J. P. Keener and J. Sneyd, *Mathematical Physiology* (Springer-Verlag, New York, 1998).
[25] E. Meron, Phys. Rep. **218**, 1–66 (1992).
[26] J. Rinzel and G. B. Ermentrout, in *Methods in Neuronal Modeling: From Ions to Networks,* edited by C. Koch and I. Segev (MIT Press, Cambridge, 1998), 2nd ed., pp. 251–291.
[27] X.-J. Wang and G. Buzsáki, J. Neurosci. **16**, 6402–6413 (1996).